Atmosphere characterization for simulation of the two optimal wireless terahertz digital communication links

Mahboubeh Mandehgar, Yihong Yang, and D. Grischkowsky*

School of Electrical and Computer Engineering, Oklahoma State University, Stillwater, Oklahoma 74078, USA
Corresponding author: daniel.grischkowsky@okstate.edu

Our studies of terahertz pulse propagation in the atmosphere have identified the two most optimal communication channels. The potential of these channels is demonstrated by physically accurate linear dispersion theory calculations of digital pulse propagation, showing it is possible to have two high-performance, point-to-point digital terahertz links in the atmosphere: a direct 95 GHz, 20 km ground link at 9.5 Gb/s with power loss of 10 dB due to water vapor at RH 58% (10 g/m^3) and 20°C, and a direct 250 GHz, geosynchronous satellite link at 20.8 Gb/s with a 2 km zenith path with water vapor loss of 9 dB. © 2013 Optical Society of America
OCIS codes: (010.1300) Atmospheric propagation; (250.0250) Optoelectronics; (300.6495) Spectroscopy, terahertz; (060.2605) Free-space optical communication.
http://dx.doi.org/10.1364/OL.38.003437

An important problem for the operating worldwide telecommunications network is to provide isolated cities and communities and remote industrial, technical, and scientific sites with wideband access to the fiber backbone [1–3]. Currently, their best access is with microwave ground links or satellite links. Another long-standing problem is to be able to provide emergency, high-bandwidth backup service for the loss of an optical fiber link. Here, we describe the potential of wireless terahertz (THz) ground links or satellite links to provide low-loss, high-bandwidth digital connections, as possible solutions to these problems [1–3].

Here, we show accurate new linear dispersion theory (LDT) calculations of THz bit pulse propagation through the atmosphere in the physically optimal communication channels I and II. The channel locations and the calculations are based on precise THz characterizations of the absorption and refractivity of the atmosphere [4,5].

As shown in Fig. 1 [5], we have recently measured the passage of transform-limited 1 ps THz input pulses with input spectra from 0.1 to 1.0 THz through a 167 m round trip optical path, where the pulse absorption and reshaping were caused by the atmospheric water vapor with RH 51% at 21°C. The stable pulseshape feature at the front of the transmitted pulse in Fig. 1(a) has propagated through the water vapor with very little spectral loss and dispersion [5]. This stable propagated pulseshape was shown to have the highlighted coherent spectrum in Fig. 1(b), which overlapped the optimal communication channels I and II.

As shown in Fig. 1(b), these optimal communication channels are defined by physical boundaries. Channel I starts with strong O_2 lines at 60 GHz and extends to the 183 GHz water vapor resonance line; channel II extends from 183 GHz to the 325 GHz water line. In order to perform LDT calculations of pulse propagation within these channels, we need accurate values of the frequency-dependent absorption and refractivity of the atmosphere. For these values, we used all knowledge to date concerning the atmosphere, and summed over the JPL database [6], for both water vapor and oxygen.

For the LDT calculations to demonstrate the excellent THz bit pulse propagation for communication links within channels I and II, we will use the ideal raised cosine input spectra [7], centered on 95 for THz link I and 250 GHz for THz link II, with FWHM bandwidths of 30 and 50 GHz, respectively, as shown highlighted in Fig. 2.

The calculated amplitude transmission from 0 to 400 GHz is shown in Fig. 2(a), for a path length of 2 km in the atmosphere at RH 57.8% (10 g/m^3) and 20°C, for van-Vleck Weisskopf (v-VW) calculations [5]
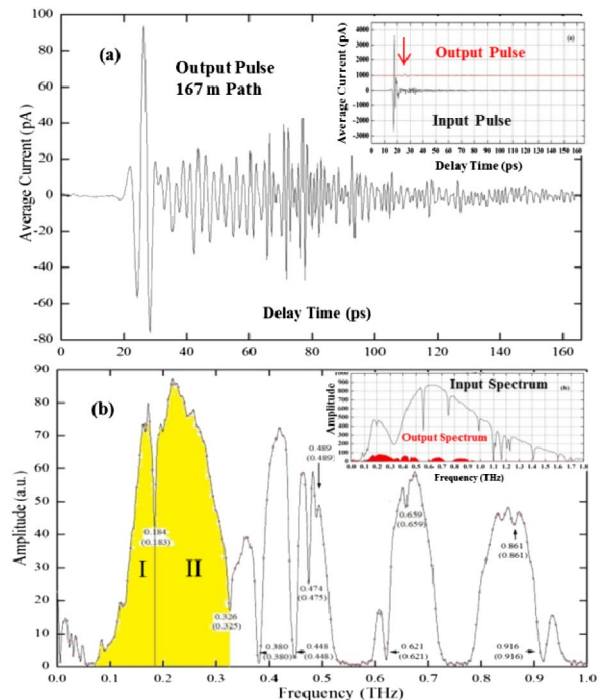

Fig. 1. (a) Transmitted THz pulse. Inset shows the input THz pulse together with the much smaller THz output pulse. (b) Amplitude spectrum of transmitted pulse. Regions I and II mark atmospheric communication channels I and II. Inset shows the input spectrum and the much smaller output spectrum.
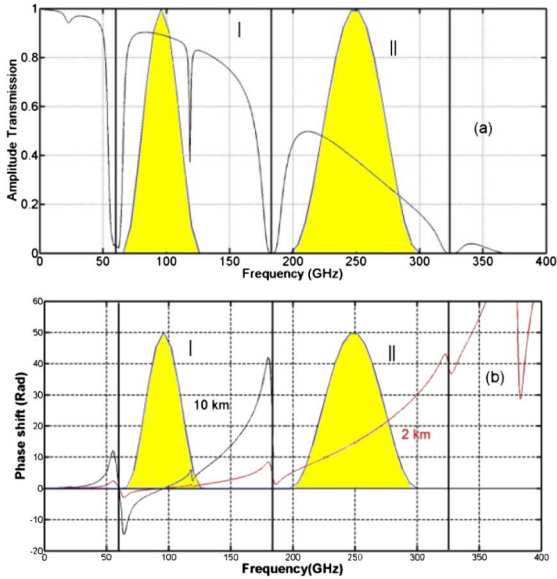
Fig. 2.   (a) Calculated amplitude transmission for a 2 km length of water vapor at RH 58% (10 g/m³) and 20°C and O₂ vapor in the atmosphere, for the van-Vleck Weisskopf (v-VW) lineshape. The calculation also includes the water continuum absorption. (b) Corresponding calculated v-VW phase in radians. For channel I, the calculated refractivity phase Φ is also shown for a 10 km length. The highlighted amplitude spectra of THz links I and II are shown with center frequencies of 95 and 250 GHz.

of water vapor with FWHM linewidths of 6.3 GHz [8], for oxygen with a cluster of approximately 25 overlapping relatively strong lines at 60 GHz with FWHM linewidths of 1.2 GHz, and for a single weak O_2 line at 120 GHz [9].

The calculation also includes the important but poorly understood water vapor continuum absorption [10–14]. For our application, the continuum absorption shown in Fig. 10 of [10] is well approximated by the simple function

$$\alpha_c(f) = \alpha_o/[1 + B \exp{-((f + 80)/69)}$$
$$- \alpha_o/[1 + B \exp{-(80/69)]}, \qquad (1)$$

for which f is the frequency in gigahertz, the parameter $B = 600$, and $\alpha_o = 2.33/\text{km}$, corresponding to the limiting power loss of 10.1 dB/km for RH 34% (H_2O density $= 5.9$ g/m³) at 20°C. For the case of Fig. 2(a), the H_2O density of 10 g/m³ required the continuum absorption to be increased, by setting $\alpha_o = 3.95$ km in Eq. (1). Figure 2(a) shows that for kilometer distances with normal values of humidity and temperature, there are no THz communication channels above the water resonance line at 325 GHz.

For Fig. 2(a), the amplitude transmissions of 2 km of the continuum obtained from Eq. (1) with $\alpha_o = 3.95/\text{km}$ are 0.95 at 95 GHz and 0.52 at 250 GHz. These transmission values were multiplied by the corresponding values for the H_2O plus O_2 vapor transmission of 0.94 at 95 GHz and 0.71 at 250 GHz, to obtain 0.89 and 0.37, respectively. The proposed links are more limited by water continuum absorption than by water and O_2 vapor absorption.

Figure 2(b) shows the corresponding v-VW phase calculation in radians for a path length of 2 km at RH 57.8%

and 20°C and oxygen. For channel I the phase is also shown for a 10 km path length.

We obtain the group velocity dispersion (GVD) for the two channels by taking the numerical second derivative with respect to the angular frequency of the phase curve in Fig. 2(b). The GVD results are presented in Fig. 3, in optical fiber units of ps²/km [7]. The two highlighted bands, located in regions of small and stable GVD, mark the THz link I centered at 95 GHz with a FWHM of 30 GHz and the THz link 2 centered at 250 GHz with a FWHM of 50 GHz. These center frequencies were chosen to minimize both absorption and GVD.

As shown in Figs. 2 and 3, channel I has significantly less absorption, less dispersion, and less GVD than channel II. Consequently, for application examples, the channel I pulses are chosen for lower frequency, lower bit rate, and longer ground link, and the channel II pulses are chosen for higher frequency, higher bit rate, satellite link, and a shorter integrated zenith path through the atmosphere [15].

The calculated propagated pulses are obtained from an LDT calculation in the frequency domain [4], using the absorption and phase displayed in Fig. 2, as shown below:

$$E(z, \omega) = E(0, \omega) \exp[i\Delta k(\omega)z] \exp[-\alpha(\omega)z/2], \qquad (2)$$

for which the input complex amplitude spectrum is given by $E(0, \omega)$, and the output complex spectrum is given by $E(z, \omega)$. The refractivity phase $\Phi = \Delta k(\omega)z$, and the amplitude transmission is $\exp[-\alpha(\omega)z/2]$. The resulting time-domain pulses are the inverse fast Fourier transform (IFFT) of the frequency-domain result $E(z, \omega)$. We have proven our LDT calculations by direct comparison with
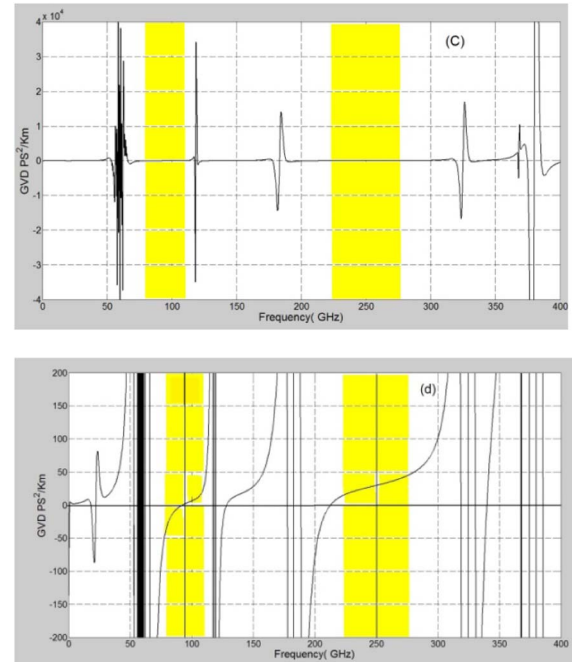

Fig. 3.   (a) GVD in ps²/km for the phase results of Fig. 2. (b) GVD results of (a) with a factor of 200 increase in vertical sensitivity show GVD = 2.44 ps²/km at 95 GHz and GVD = 29.7 at 250 GHz. The highlighted bands mark the ground link at 95 GHz and the satellite link at 250 GHz.
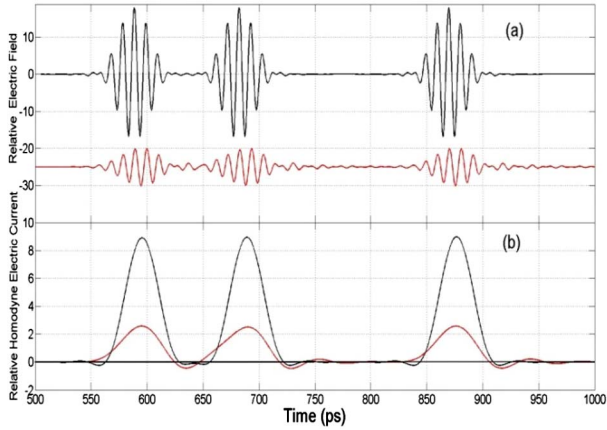
Fig. 4. (a) Channel I: input transform-limited THz "one" bit pulses (black larger pulses) and the calculated smaller, red output pulses after 20 km propagation in the atmosphere with RH 58% (10 g/m^3) and 20°C. (b) Calculated homodyne detected input upper black current pulses and the output lower red pulses, clearly showing the (1101) bit sequence.

excellent agreement with measured transmitted pulses with propagation distances of 6.18 and 137 m [5].

In order to characterize our communications channel I [7], a propagation calculation for three transform-limited, THz "one" bit pulses of the channel I ground link is shown in Fig. 4(a), before and after passage through 20 km of atmosphere with water vapor at RH 58% (10 g/m^3) and 20°C. The symmetry of the input pulses shows that they are transform-limited with the envelope determined by the raised cosine spectrum [7]. After 20 km of propagation in the atmosphere the pulses are attenuated and slightly broadened with some loss of symmetry due to GVD, although the center frequency and bandwidth were chosen to minimize these effects. However, they are still well resolved and would allow good bit recognition.

This almost undistorted 20 km digital pulse propagation is consistent with the initial observation shown in Fig. 1 of the undistorted pulse propagation of the feature at the front of the strongly reshaped main pulse. The feature was shown to have a spectrum overlapping channels I and II [5].

For applications, these coherent bit pulses were changed to current pulses by simulating homodyne detection with a 95 GHz (period of 10.5263 ps) local oscillator (LO), and using a power detector. For coherent detection, the bit separation is nine LO periods equal to 94.737 ps, corresponding to the bit rate of 9.5 Gb/s. The calculated current bit pulses were obtained from the homodyne low frequency component centered on zero frequency with a FWHM of 30 GHz. The resulting "one" bit pulses shown in Fig. 4(b) are ideal for digital electronics, as shown by their well-resolved four bit sequence (1101).

The proposed THz ground link transmitter with a 2 m dish antenna operating at 95 GHz would have a diffraction-limited beam power diameter of 28.4 m at 20 km. The power transfer between the two 2 m antennas is given by the ratio of the area of the 2 m receiving antenna to that of the diffraction-limited beam $(2 \text{ m}/28.4 \text{ m})^2 = 4.96 \times 10^{-3}$, corresponding to the diffraction propagation loss of 23.0 dB. The full angular beam power divergence is

1.4 mrad, compared to the human eye with a resolution angle of 0.29 mrad. Consequently, an optical sight could enable the initial alignment between the two antennas.

An important demonstration of a custom-built Nippon Telegraph and Telephone Corporation (NTT) prototype wireless system [2] was the 800 m wireless transmission trial of the live television broadcast coverage of the Beijing 2008 Olympics [2]. The transmitted power of 10 mW of the 120 GHz band with 10 GbB (10.3125 Gb/s) had simple amplitude shift keying, and the receiver sensitivity was −35 dBm for a bit error rate of less than 10^{-12} [2].

The NTT system would be capable of driving the proposed 20 km link, using 2 m dish antennas, but with a change to the optimal carrier frequency of 95 GHz for lower absorption and minimal GVD. The total of the atmospheric loss of 10 dB and the diffraction loss of 26 dB for our 20 km link is 34 dB, giving the proposed system a power margin of 9 dB, for a transmitted power of 10 mW.

A similar propagation calculation for three transform-limited, channel II, THz "one" bit pulses with a center frequency of 250 GHz to minimize both loss and GVD is shown in Fig. 5(a), before and after passage through 2 km of atmosphere with water vapor at RH 58% and 20°C (equivalent to the zenith integration) [15]. Compared to the channel I performance, these channel II pulses clearly show both higher attenuation and much increased GVD. The transmitted bit pulses have broadened so that they are starting to overlap and they have significant asymmetry, even though their central frequency is at the optimal location on the GVD curve with an appropriate bandwidth.

These coherent bit pulses were also changed to current pulses by simulated homodyne detection with a 250 GHz (period of 4 ps) LO. The bit separation is 12 LO periods equal to 48.000 ps, corresponding to the bit rate of 20.833 Gb/s. The resulting "one" bit pulses shown in Fig. 5(b) are ideal for digital electronics.

The proposed channel II THz link to a geosynchronous (GEO) communications satellite approximately 35 800 km above sea level has several important features compared
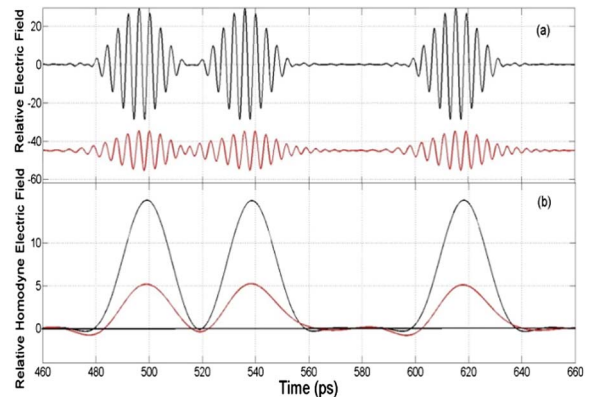

Fig. 5. (a) Channel II: input transform-limited THz "one" bit pulses II (black larger pulses) and the calculated smaller, red output pulses after 2 km propagation in the atmosphere with RH 58% and at 20°C (equivalent to zenith integration) [15]. (b) Calculated homodyne detected input upper black current pulses and the output lower red pulses, clearly showing the four bit sequence (1101).

to existing satellite links. Using a 5 m diameter antenna for the earth gateway antenna, the diffraction-limited beam power diameter at the satellite would be only 2.57 km. The power transfer between the 5 m ground antenna and the 2 m satellite antenna is given by the propagation loss of only 62.1 dB, compared to 90 dB for a 10 GHz microwave system with a 20 m Gateway antenna and a 2 m satellite antenna. The full angular 250 GHz beam power divergence is 0.072 mrad, requiring an achievable pointing accuracy and stability four times better than the human eye. A feature of this alignment precision is secure point-to-point communications.

It is important to note that this work is contained within the millimeter-wave domain, also designated as the extremely high frequency (EHF) domain extending from 30 to 300 GHz [3]. The proposed channel I, THz ground link with center frequency of 95 and 30 GHz FWHM bandwidth essentially fills the EHF-W band with boundaries from 75 to 110 GHz [3]. The channel II, THz GEO satellite link with center frequency of 250 GHz is also within the EHF domain.

At the present time no operative *W*-band communication systems have been developed [3], and there is no commercial activity from the *W* band up to 300 GHz, the high frequency limit of the EHF range. The *W* band is currently considered as the frontier for space telecommunications.

Our results, which can enable many applications, have demonstrated the importance of the center frequency of wide-band allocations for optimized digital communications in the THz (EHF) frequency range [3], for which crosstalk is much reduced due to the line-of-sight nature of the THz links.

In summary, by combining recent measurements with the latest physical understanding of the atmosphere and using the extensive JPL and (HITRAN) databases, we have presented, to our knowledge, the most comprehensive description of the absorption, dispersion, and GVD from 0.06 to 1 THz to date, and have thereby located the two optimum communication channels in the atmosphere. The performance of these channels was demonstrated by the simulated transmission of digital pulses through the channels, using LDT, based on the accurate absorption, dispersion, and GVD description of the atmosphere. Channel I was demonstrated to enable a

THz ground link with a center frequency of 95 GHz and FWHM bandwidth of 30 GHz that could transmit 9.5 Gb/s through 20 km of standard atmosphere. Channel II enabled a THz (GEO) satellite uplink with a center frequency of 250 GHz and a FWHM bandwidth of 50 GHz that could transmit 20.8 Gb/s through the atmosphere.

These channels with minimum loss and GVD were chosen to optimize their performance to transmit digital data, without regard for frequency band boundaries and bandwidth allocations. The properties of these channels should stimulate field testing and development, and serve as a guide to future frequency allocations.

References

1. J. Wells, IEEE Microw. Mag. **10**(3), 104 (2009).
2. T. Kosugi, A. Hirata, T. Nagatsuma, and Y. Kado, IEEE Microw. Mag. **10**(2), 68 (2009).
3. E. Cianca, T. Rossi, A. Yaholom, Y. Pinhasi, J. Farserotu, and C. Sacchi, Proc. IEEE **99**, 1858 (2011).
4. Y. Yang, A. Shutler, and D. Grischkowsky, Opt. Express **19**, 8830 (2011).
5. Y. Yang, M. Mandehgar, and D. Grischkowsky, IEEE Trans. THz Sci. Technol. **2**, 406 (2012).
6. H. M. Pickett, R. L. Poynter, E. A. Cohen, M. L. Delitsky, J. C. Pearson, and H. S. P. Muller, J. Quant. Spectrosc. Radiat. Transfer **60**, 883 (1998).
7. G. P. Agrawal, *Fiber-Optic Communication Systems*, 3rd ed. (Wiley, 2002).
8. S. D. Gasster, C. H. Townes, D. Goorvitch, and F. P. J. Valero, J. Opt. Soc. Am. B **5**, 593 (1988).
9. M. W. P. Strandberg, C. Y. Meng, and J. G. Ingersoll, Phys. Rev. **75**, 1524 (1949).
10. D. E. Burch and G. A. Gryvnak, in *Proceedings of the International Workshop on Atmospheric Water Vapor* (Academic, 1980), pp. 47–76.
11. H. J. Liebe, Int. J. Infrared Millim. Waves **5**, 207 (1984).
12. P. W. Rosenkranz, Radio Sci. **33**, 919 (1998).
13. I. V. Ptashnik, K. P. Shine, and A. A. Vigasin, J. Quant. Spectrosc. Radiat. Transfer **112**, 1286 (2011).
14. D. M. Slocum, E. J. Slingerland, R. H. Giles, and T. M. Goyette, "Atmospheric absorption of terahertz radiation and water vapor continuum effects," J. Quant. Spectrosc. Radiat. Transfer **127**, 49 (2013).
15. R. K. Crane, Proc. IEEE **59**, 173 (1971).